

Infrared-based ridge waveguide lasers for wavelength division multiplexing applications

L. Davis, M. Mazed, S. Keo, J. Singletary, T. Vang, S. Forouhar

Center for Space Microelectronics, Jet Propulsion Laboratory
California Institute of Technology
Pasadena, CA 91109 USA

ABSTRACT

Wavelength division multiplexed (WDM) systems place stringent requirements on the absolute wavelength and wavelength spacing of the elements in laser arrays. Ridge waveguides (RW) show excellent potential for practical implementation due to their simple fabrication with relaxed fabrication tolerances, high reliability and good performance. An analysis of the fabrication tolerances for RW and buried heterostructure (BH) devices is performed, showing the advantages offered by the ridge design. The performance limitations that are common to both BH and RW devices will be discussed. Experimental results for four element distributed feedback (DFB) ridge laser arrays at 1.55 μm will be presented as well.

Keywords: wavelength division multiplexing, ridge waveguide laser, buried heterostructure laser, semiconductor laser array, distributed feedback laser

1. INTRODUCTION

The development of low-loss, low dispersion silica-based fiber and high speed semiconductor optical sources and photodetectors has resulted in photonics dominating long haul point-to-point transmission systems. The tremendous bandwidth capacity of optical fibers, however, is largely untapped by today's networks, due to the speed limitations of electronics in the data path. Present long haul communications is dominated by transmission at 1.55 μm ; silica fibers have a low loss region around this wavelength of $> 100 \text{ nm}$ (13 THz).

Data and telephony communications are continuously pushing for increased transmission bandwidth. WDM is a powerful technique to increase the bandwidth of present communications systems through the simultaneous transmission of two or more signals at different optical wavelengths over the same fiber. By utilizing multiple channels, each at a moderate bit rate and on a separate wavelength, a very large aggregate bit rate can be achieved (N wavelengths \times bit rate). The use of Erbium-Doped Fiber Amplifiers (EDFAs) will limit the available bandwidth of the fibers around 1.55 μm to the gain bandwidth of the amplifier ($\sim 47 \text{ nm}$ or 5.9 THz), which is still capable of holding > 40 channels (assuming a 100 GHz channel allocation). Thus WDM allows one to better access the tremendous bandwidth of optical fibers while still allowing the transmitters and receivers to operate at the single-channel transmission rate.

Sources for WDM communication systems have been the subject of much research. DFB lasers are utilized because of their superior performance and wavelength stability versus Fabry-Perot (F-P) and distributed Bragg reflector (DBR) lasers for long haul, high bit rate communications. The sources for a multi-wavelength transmitter can be attained by screening individual devices; however, there is a high cost and low yield associated with this method. The use of laser arrays, where all the emitters are located on the same chip, offer an advantage in packaging (single package for all the devices) as well as offering the potential for further integration with drivers, integrated optics, amplifiers, etc.

The difficulty in the use of laser arrays comes in the precise definition of the wavelength of each element in the laser array. In a DFB laser, the final emission wavelength of the device is set by the Bragg condition, $\lambda = 2 n_m A$, where n_m is the modal index and A is the pitch of the DFB grating. Control of the emission wavelength requires absolute control of the grating pitch and the modal index. The systematic variation of the emission wavelength across a laser array can be achieved by variation of either the grating pitch or the modal index. The grating pitch is more controllably varied, and arrays generated by varying the grating pitch have been demonstrated using direct write e-beam lithography, step-and-repeat holography, binary phase mask lithography and x-ray lithography. Systematic variation of the modal index has been achieved through ridge width variation selective area epitaxy and on-chip heaters.

DFB laser arrays typically consist of either BH or RW structures. Impressive results have been seen for both BH and RW lasers in terms of threshold, efficiency and reliability; however, BH lasers are more commonly employed due to their reduced leakage, better current confinement and higher single mode power. However, for absolute wavelength control the fabrication tolerances for BH lasers are more stringent than for RW lasers, due to the generally narrower active region and large index difference around the active region. In this paper, an analysis of the fabrication tolerances for RW and BH devices is performed, showing the advantage offered by the ridge design. The wavelength control limitations that are common to both buried heterostructure and RW devices are also discussed. Section 2 consists of simulation results showing the effect of various fabrication parameters on the final emission wavelength of RW and BH lasers. In Section 3, the performance of RW lasers for a specific WDM application is discussed, Section 4 finishes with the conclusions.

2. SIMULATION RESULTS

The absolute wavelength and wavelength spacing of the elements in the laser arrays is critical for system level performance. Systems requirements have specified wavelength control as tight as ± 0.2 nm for a given channel so that the wavelength of the transmitter signal and the passband of the demultiplexing element at the receiver end are properly aligned. Using e-beam lithography or an e-beam generated binary phase mask, the grating pitch can be very precisely set to $< 1\text{\AA}$ tolerance. While systematic variations in the modal index can be used to precisely set the different wavelengths for each channel, it is the non-systematic variation in the modal index that causes the greatest yield hit in the wavelength registration. Since the final emission wavelength of a DFB laser is directly proportional to the modal index from the Bragg condition, any variation in the modal index will have an effect on the emission wavelength. While temperature tuning can be used to move the wavelengths of all the elements in an array equally, temperature tuning can not easily be used to compensate for inaccurate wavelength spacing of the elements within an array. Consequently, the critical factors in the fabrication of WDM DFB laser arrays are those which affect the device-to-device wavelength spacing. An empirical formulation for the variation in the emission wavelength of a DFB laser can be written as

$$\Delta\lambda = 2 \Delta n_m, \Delta n_m \approx (\partial n / \partial w) dw + (\partial n / \partial t) dt + (\partial n / \partial P) dP + (\partial n / \partial g) dg + (\partial n / \partial B) dB + \Delta\lambda_m \quad (1)$$

where w is the ridge width; t is the layer thicknesses; P is the PL wavelength (material composition) of the layers; g is the modal gain at the emission wavelength; B is the DFB grating etch depth; and $\Delta\lambda_m$ relates to the mode spacing in an intrinsically dual mode DFB laser.

The lasers modeled in this paper are separate confinement heterostructure (SCH) type designs, consisting of the following layers: n -InP substrate, 100 nm InGaAsP ($\lambda = 1.2 \mu\text{m}$) SCH layer, an active region of six 7.0 nm InGaAsP quantum wells separated by five 9.0 nm InGaAsP ($\lambda = 1.2 \mu\text{m}$) barriers, 100 nm InGaAsP ($\lambda = 1.2 \mu\text{m}$) SCH layer, 0.23 μm InP spacer layer, 80.0 nm InGaAsP ($\lambda = 1.18 \mu\text{m}$) etch stop layer, and 1.3 μm p -InP. The etch stop layer is required for the RW lasers to control the ridge depth and thus the A_n . The same layer structure was used in our BH simulation for consistency. To mimic real devices as closely as possible, the following assumptions were made in our calculation: (1) the grating is etched into the top SCH layer; (2) polyimide with a refractive index of 1.75 at 1.55 μm was used to planarize the RW device, and InP was used to bury the BH device; (3) the semiconductor indices of refraction were calculated from Ref. [15]; and (4) the typical active region (ridge) widths of 1.0 μm and 3.0 μm are assumed for the BH and RW devices, respectively. The modeling was conducted using the effective index method. Although this calculation ignored the effects of propagation losses as well as the doping and carrier-induced index changes, a reasonable agreement was achieved with experimental results. Furthermore, the results shown here provide the trends and relative magnitudes of the modal index changes produced by various perturbations in the device design and fabrication.

The first term in equation (1), the width variation, dominates the variation of the modal index. Fig. 1 shows the modal index variation for both BH and RW lasers as a function of active layer [ridge] widths - it is the slope of these curves that gives the sensitivity of the laser emission wavelength to the width. For a variation of $\pm 0.1 \mu\text{m}$ in the width (produced by lithographic and etch limitations), the BH laser emission will be ± 1.3 nm, and the RW laser will be ± 0.1 nm (Table 1 shows the relative size of all the discussed effects). This result reveals an important problem with employing BH lasers as WDM transmitters in an array, and demonstrates the advantage that RW lasers have for WDM array applications. The large A_n in BH lasers requires a narrower mesa to keep BH lasers single mode, which means that a given size variation in the BH width will have a larger percentage change in the BH width and thus have a larger effect on the modal index than the same variation will have in a RW laser. Furthermore, the larger A_n in BH lasers gives the BH laser a larger slope at all widths in Fig. 1,

Effect	Typical variation	Modal index effect (x 10 ⁴)				Wavelength effect (nm)			
		BH		RW		BH		RW	
dW	± 0.1 μm	7.6	27.6	1.6	1.6	1.3	1.3	0.1	0.1
dt	± 1%	7.7	5.7	7.7	7.7	0.27	0.27	0.37	0.37
dλ _g	± 5 nm	6.6	-	58.5	8.5	0.31	0.31	0.41	0.41
dg	± 20/cm	-	-	-	-	0.24	0.24	0.24	0.24
dB	± 10 nm	7.7	4.7	6.1	6.1	0.23	0.23	0.29	0.29
Δλ _g	-	-	-	-	-	1.2	1.2	1.2	1.2

Table I. Effect of process variations on the final emission wavelength of 1.0 μm BH and 3.0 μm RW lasers, using $\Delta\lambda = 2 \Delta n_m A$ and $A = 240.0$ nm,

The other growth and processing related effects represented in Eqn. (1) are similar for RW and BH devices, and contribute effects that are much smaller. Growth non-uniformities across a wafer and from wafer-to-wafer - leading to thickness and composition variations - also cause a change in the modal index of a laser. The effect of layer thickness variation on the modal index was calculated versus the percentage change in the layer thicknesses, from -10% to +10% (all the layer thicknesses in the structure were changed). The results for both BH and RW lasers were linear over this thickness variation. For a 3 μm RW and a 1 μm BH, the modal index changes by 7.7×10^{-4} and 5.7×10^{-4} for each 1% change in the layer thicknesses, respectively. The resulting wavelength change at 1.55 μm would be (using $\Delta\lambda = 2 \Delta n_m A$, and $A = 240.0$ nm) -0.37 nm for a RW laser, and -0.28 nm for a BH laser. Compositional changes to the quaternary guiding layers will also produce changes in the modal index. The composition of the $\lambda = 1.2$ μm InGaAsP SCH layers were varied from $\lambda = 1.19$ μm to $\lambda = 1.21$ μm in our model, and the effect on the final modal index determined. Over this range, the modal index variation is linear with composition change. The modal index of a 3.0 μm RW laser changes 1.7×10^{-4} per nanometer wavelength change in composition, and for a 1.0 μm BH laser the change is 1.3×10^{-4} per nanometer. Compositional changes to the active layers, which are very thin, have only a small effect directly on the modal index. However, compositional variations in the active layers can lead to gain variations, which cause (through the Kramer-Kronig relations) modal index variations¹⁷. The variation in the modal index with threshold gain variations can be expressed as¹⁷

$$\Delta\lambda = \lambda^2 \alpha \Delta g_{th} / 4 \pi n_m \quad (2)$$

where g_{th} is the threshold gain, and a is the linewidth enhancement factor. As an estimate of the size of this effect, using $a = 2$ and $\Delta g_{th} = 20/\text{cm}$, $\Delta\lambda \sim 0.24$ nm for both BH and RW lasers.

The control of the DB grating depth is typically of the order of ± 10.0 nm. This variation in the etch depth leads to a variation in the modal index. The modal index of a 3.0 μm RW laser changes 6.1×10^{-5} per nanometer change in etch depth, and for a 1.0 μm BH laser the change is 4.7×10^{-5} per nanometer, which is significant. Alternative designs with less sensitivity to the grating depth alleviate the dependence of the emission wavelength on the grating etch depth accuracy¹⁸.

The other large term in Eqn. (1) is $\Delta\lambda_{sp}$, which is the nominal spacing between the intrinsic dual modes of the DB¹⁹. The stop band width can be calculated from the approximate expression found in¹⁹

$$\kappa L = \pi/2 (\Delta\lambda_{sp} / \Delta\lambda_{FP} - \Delta\lambda_{sp} / \Delta\lambda_{sp}) \quad (3)$$

where κL is the grating coupling coefficient and $\Delta\lambda_{FP}$ is the Fabry-Perot mode spacing. For a device with a κL of 1-2 and a cavity length of 300 μm, the $\Delta\lambda_{sp}$ is 1-2 nm. Since the emission wavelength of the DB laser must be controlled to ~ 0.2 nm to fit in pre-assigned channel allocations in a WDM system, this uncertainty in the emission wavelength is not tolerable. A method must be used to deterministically set the Bragg mode that lases. A significant amount of research has successfully pursued the use of either phase-shifted²⁰ or complex-coupled devices²¹ to precisely set the lasing mode. Both types of devices remove the dual mode degeneracy found in standard DBs and have only a single DB lasing mode.

A number of factors affect the modal index, and thus the emission wavelength, of semiconductor lasers. Both RW and DBL lasers are affected by a number of processing and growth related variations. Phase-shifted or complex-coupled gratings can be used to avoid the wavelength uncertainty found in dual mode DBL lasers; and a separate grating layer (away from the active region) can solve the grating etch difficulty. The other processing and growth related parameters are unavoidable; however, through careful optimization of device fabrication, the effect of these other parameters can be minimized. While the variations discussed can cause significant wavelength shifts across a wafer and from wafer-to-wafer, over small areas the variations should be smaller, allowing for a reasonable yield. Looking at table 1, all the effects can cause wavelength variations > 0.2 nm. However, over the small wafer area occupied by a single array, the device-to-device variation should be small; from one array to another, it may be significant, requiring temperature tuning to bring one laser array output into alignment with another. As the width variation in the waveguides is seen to be the largest source of variation in the emission wavelength, the reduced dependence on the width found in RW devices makes a strong case for their use in WDM DBL laser arrays.

3. EXPERIMENTAL RESULTS

JPL's development of WDM is intended for a state of the art all-optic terabit computer network linking supercomputers to create a massively parallel computing capability²³. WDM is the key to making such a network operational. The first generation system requires 4 wavelength channels with $\Delta\lambda = 4 \pm 1$ nm; the next generation will be 10 elements with 2nm spacing.

The arrays for this computer network are 4 element DBL RW laser arrays. The laser wafers were prepared by atmospheric pressure metal-organic chemical vapor deposition (MOCVD) on (100)-oriented InP substrates. The active region consists of 4 compressively strained ($\epsilon = 1\%$) InGaAsP quantum wells, each 94 Å wide, with 150 Å barriers of InGaAsP ($\lambda = 1.2 \mu\text{m}$). The optical confinement is provided by a stepped separate confinement heterostructure (SCH) region consisting of 900 Å InGaAsP ($\lambda = 1.2 \mu\text{m}$) and 800 Å InGaAsP ($\lambda = 1.15 \mu\text{m}$), with InP as the top and bottom cladding material. The conduction band profile of the complete laser structure is shown in Fig. 1. Broad area lasers were fabricated to evaluate the quality of the material; measurement of the threshold current and slope efficiency versus cavity length allowed the extraction of the internal quantum efficiency (60 %) and the internal loss (17.4 /cm).

Fabrication of this material into 4 element DBL laser arrays requires e-beam writing of the diffraction gratings, an MOCVD regrowth, and the fabrication of the ridge waveguide structure. The top 4 layers of the laser structure (contact, 2 InP layers, and etch stop in Fig. 2) are removed in order to define the distributed feedback grating in the SCH region. The pitch of the grating for the individual lasers is determined by the calculated modal index and the design criteria of 4 wavelengths from 1.54-1.56 μm ; this leads to 4 grating pitches in the range from 2375 - 2400 Å. The base wafer was designed to have the gain peak to the long wavelength side of 4 wavelengths for improved differential gain and reduced linewidth enhancement factor²⁴, with the shortest wavelength being 25 - 30 nm from the gain peak. The gratings are defined by direct write e-beam in PMMA, and etched into the InGaAsP (1.15 μm) layer using an aqueous solution of HBr and HNO_3 . MOCVD is then used to regrow the same 4 layers back onto the structure. Ridge waveguide lasers are then fabricated from this regrown structure. First, the p contact (Ti/Pt/Au) is deposited and annealed; each contact is 3.5 μm wide. A self-aligned wet chemical etch is used to define the ridge waveguide structure. Use of an etch stop allows for reproducible waveguide definition with a pre-determined amount of index-guiding; the amount of index-guiding is dictated by the InP spacer thickness. After the ridge definition etch, polyimide is applied to the wafer and then cured. Oxygen-based reactive ion etching (RIE) is used to open the polyimide to the p contact. The final top side processing is the lithography and evaporation for the contact metal (Cr/Au). The wafer is then lapped to a thickness of $\sim 100 \mu\text{m}$, and then a back contact metal is evaporated (Ni/AuGe/Ti/Au). A final anneal completes the laser fabrication, and the devices are then scribed and cleaved. A cavity length of 300 μm is chosen for speed and optimal κL of the grating. The devices are AR coated on one side (other side as-cleaved) to improve the single mode yield and suppress the 1-P modes which would otherwise last in the devices with DBL modes far (15-25 nm) from the gain peak.

The devices are soldered to a copper submount for CW operation. The laser spacing (250 μm) is designed to be compatible with silicon v-groove based fiber arrays. The light vs. current characteristics of a 300 μm long, 4 element laser array is shown in Fig. 3(a), showing the uniformity of the threshold and slope efficiency of the devices. Fig. 3(b) shows the spectral characteristics of this same array for a drive current of 50 mA, displaying a side mode suppression ratio greater

than 20 dB. The finished laser arrays have wavelength separations of 4-5 nm, very uniform threshold currents as low as 15 mA, output power of several mW, and good sidemode suppression ratios.

The wavelength separation and the absolute wavelength of the lasers is very important to the final system performance. Shown in Fig. 4 is the wavelength spread for a few arrays from the same process run. These devices meet the required wavelength specifications. Looking at all the array chips in a given run, the wavelength spread in our devices is -1.0 nm at a given grating pitch. Subthreshold measurement of the spectrum shows that this is predominantly due to dualmode nature of the DFB lasers, with the mode on either Side of the stop band equally likely to lase. Thus it is the stop band width that dominates the spread in the wavelength, and alternative devices (complex coupled, $\lambda/4$ -shifted) are being pursued to avoid this phenomena. Another effect that must be considered is thermal crosstalk - the change in the lasing wavelength as the other lasers in the array are modulated or turned on/off. Fig. 5 shows the effect on a device if the adjacent laser (250 μm away) is current swept, and if the furthest device in the array (750 μm away) is swept. While the thermally induced wavelength change is not too large for this system demonstration, for very small channel separations in larger arrays in future WDM systems thermal crosstalk may be a concern.

4. CONCLUSIONS

An analysis of the fabrication tolerances for BH and RW lasers was performed, showing the fabrication induced wavelength variations present in these types of devices. The stringent requirements for wavelength spacing and absolute wavelength in WDM systems demand careful control of the growth and processing steps. With performance results nearly equal to BH lasers, the reduced width dependence in RW lasers makes a strong case for their use in WDM DFB laser arrays. RW laser arrays were shown to provide the required wavelength accuracy for a high capacity WDM system.

5. ACKNOWLEDGMENTS

The authors would like to acknowledge the help of Prof. H. Temkin, Colorado State University, in the characterization of the array devices. The research described in this paper was performed by the Center for Space Microelectronics Technology, Jet Propulsion Laboratory, California Institute of Technology, and was sponsored by Ballistic Missile Defense Organization / Innovative Science and Technology Office (BMDO/IST), through an agreement with the National Aeronautics and Space Administration.

6. REFERENCES

1. Charles A. Brackett, "Dense Wavelength Division Multiplexing Networks: principles and Applications," *IEEE J. on Selected Areas in Comm.*, vol. 8, no. 6, 948-964, 1990.
2. G.P. Agrawal and N.K. Dutta, *Semiconductor Lasers*, Second Ed., Van Nostrand Reinhold, New York, 1993.
3. T. Koch and Uziel Koren, "Photonic Integrated Circuits," *Technical Journal*, January/February 1992, 63-74.
4. B. James Ainslie, "A Review of the Fabrication and Properties of Erbium-Doped Fibers for Optical Amplifiers," *IEEE J. of Lightwave Tech.*, vol. 9, no. 2, 220-227, 1991.
5. T. Koch, "Laser Sources for Wavelength Division Multiplexing," *Conference on Optical Fiber Communications (OFC)*, WFI, San Diego, CA, Feb. 1995.
6. G.P. Li, T. Makino, A. Sarangan, W. Huang, "16-Wavelength Gain-Coupled DFB Laser Array with Fine Tunability," *IEEE Photon. Tech. Lett.*, VOL 8, 22-24, 1996.
7. C.E. Zah, P.S. Li, F. Favire, B. Pathak, R. Bhat, C. Canau, A.S. Gozdz, N.C. Andreadakis, M.A. Koza, T.P. Lee, T.C. Wu, K.Y. Lau, "1.5 μm Compressive-Strained Multiquantum Well 20-Wavelength Distributed-Feedback Laser Arrays," *Electron. Lett.*, vol. 28, 824-826, 1992.
8. M.G. Young, U. Korea, B.I. Miller, M.A. Newkirk, M. Chien, M. Zirgibi, C. Dragone, B. Tell, H.M. Presby, G. Raybon, "A 16x1 Wavelength Division Multiplexer with Integrated Distributed Bragg Reflector Lasers and Electroabsorption Modulators," *IEEE Photon. Tech. Lett.*, vol. 5, 908-910, 1993.
9. M. Okai, S. Tsuji, N. Chinone, T. Harada, "Novel Method to Fabricate Corrugation for a $\lambda/4$ -Shifted Distributed Feedback Laser using a Grating Photomask," *Appl. Phys. Lett.*, vol. 55, 415-417, 1989.
10. M. Nakao, K. Sale, I. Nishida, T. Tamamura, "Distributed Feedback Laser Arrays Fabricated by Synchrotron Orbital Radiation Lithography," *IEEE J. of Selected Areas in Comm.*, vol. 8, 1178-1182, 1990.

11. Y. Katoh, I. Kunii, Y. Matsui, H. Wada, I. Kamijoh, Y. Kawai, "DBR Laser Array For WDM System," *Electron. Lett.*, vol. 29, 2195-2197, 1993.
12. L.A. Wang, Y.H. Lo, A.S. Gozdz, P. S.D. Lin, M.Z. Iqbal, R. Bhat, "Integrated Four-Wavelength DFB Laser Array with 10Gb/s Speed and 5 nm Continuous Tuning Range," *IEEE Photon. Tech. Lett.*, vol. 4, 318-321, 1992.
13. G.P. Agrawal and N.K. Dutta, Semiconductor Lasers, 2nd edition, Van Nostrand Reinhold, New York, 1993, ch. 5.
14. W. Young, "WDM Laser Array Packaging: Electrical and Optical Issues," *Lasers and Electro-Optics Society (LEOS) conference*, Oct. 95, OPMR4, 1.
15. GaInAsP Alloy Semiconductors, ed. by T.P. Pearsall, John Wiley & Sons, Ltd., 1982, 362.
16. C.H. Henry, "Theory of the Linewidth of Semiconductor Lasers," *IEEE J. of Quant. Electron.*, vol. 18, no. 2, 1982, 259-264.
17. Y. Kotaki and I. Ishikawa, "Wavelength Tunable DFB and DBR Lasers for Coherent Optical Fibre Communications," *IEEE Preceding. ~ -J*, vol. 138, no. 2, 1991, 171-177.
18. A. Takemoto, Y. Ohkura, Y. Kawana, Y. Nakajima, T. Kimura, N. Yoshida, S. Kakimoto and W. Susaki, "1.3 μm Distributed Feedback Laser Diode with a Grating Accurately Controlled by a New Fabrication Technique," *IEEE J. of Lightwave Tech.*, vol. 7, 2072-2077, 1989.
19. H. Kogelnik and C.V. Shank, "Coupled Wave Theory of Distributed Feedback Lasers," *J. Appl. Phys.*, vol. 43, 1972, 2327-2335.
20. L.L. Ketelsen, I. Hoshino and D.A. Ackerman, "Experimental and Theoretical Evaluation of the CW Suppression of "Side Modes in Conventional 1.55 μm InP-InGaAsP Distributed Feedback Lasers," *J. of Quant. Electron.*, vol. 27, no. 4, 1991, 965-975.
21. M.G. Young, T.J. Koch, U. Koren, D.M. Tennant, B.J. Miller, M. Chien and K. Feder, "Wavelength Uniformity in $\lambda/4$ shifted DFB laser array WDM transmitters," *Electron. Lett.*, vol. 31, no. 20, 1995, 1750-1752.
22. G.P. Li, I. Makino, R. Moore and N. Puetz, "1.55 μm Index/Gain Coupled DFB Lasers with Strained Layer Multiquantum-Well Active Grating," *Electron. Lett.*, vol. 28, no. 18, 1992, 1726-1727.
23. S.I. Monacos, J.M. Morookian, L. Davis, L.A. Bergman, S. Forouhar, J.R. Saucier, "All-Optical WDM Packet Networks," accepted to *IEEE Journal of Selected Areas in Communications*.
24. J. Yamanaka, Y. Yoshikuni, W. Iui, K. Yokoyama, S. Seki, "Potential Chirpless DFB Lasers for InGaAs/InGaAsP Compressive-Strained Quantum Wells Using Modulation Doping," *IEEE Photon. Tech. Lett.*, vol. 4, 1318-1321, 1992.
25. C.H. Henry, "Performance of Distributed Feedback Lasers Designed to Cover the Energy Gap Mode," *IEEE J. of Quant. Electron.*, vol. 21, 1913-1918, 1985.

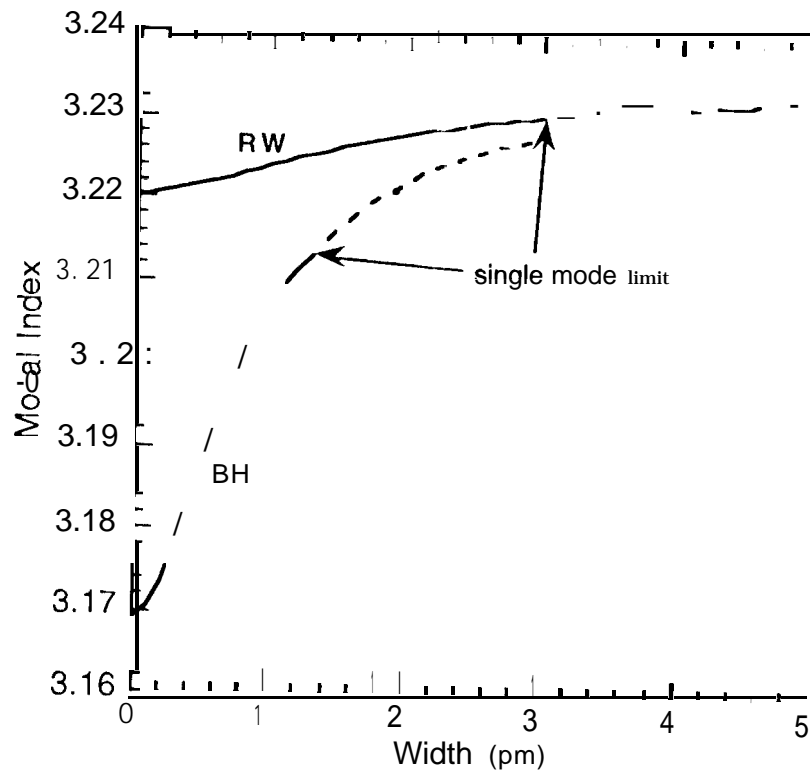


Figure 1. Modal index versus device width for BH and RW lasers. Note the much larger slope for the BH devices at all widths.

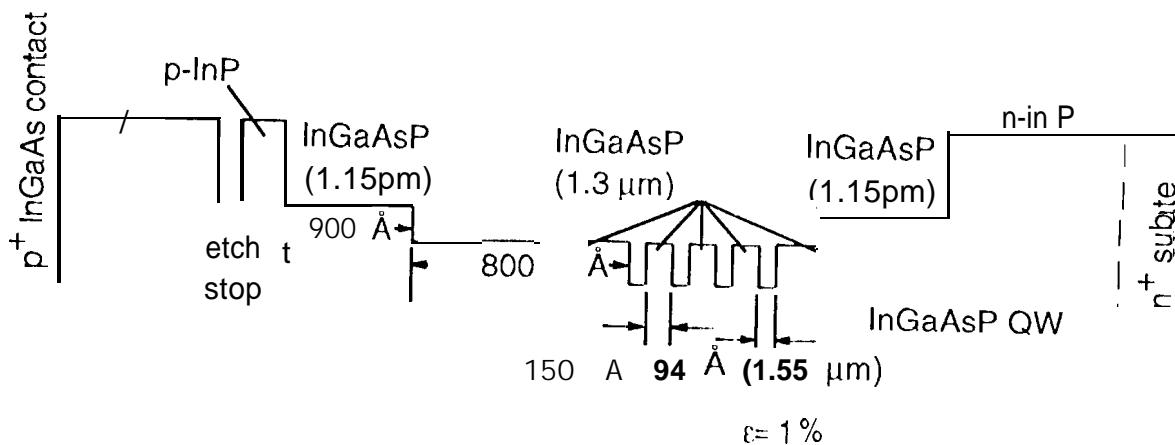


Figure 2. Layer structure schematic of the InP-based ridge waveguide laser.

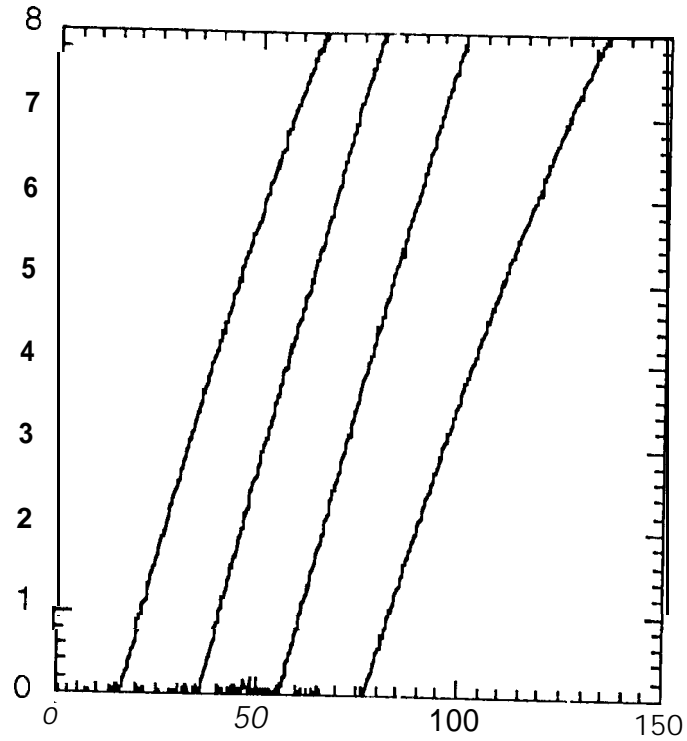


Figure 3(a). L-1 characteristics of a typical 4 element DFB array; the ordinate is shifted by 20 mA between devices.

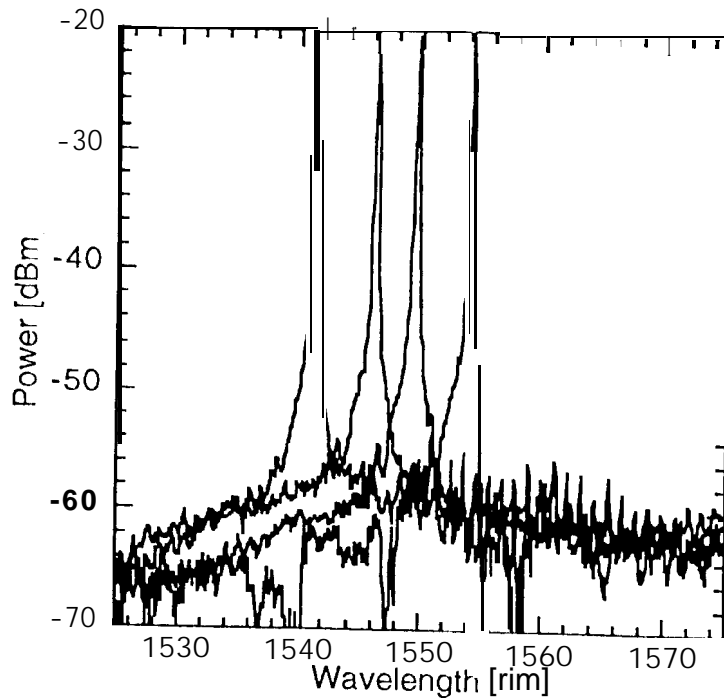


Figure 3(b). Spectral characteristics of the 4 element DFB array.

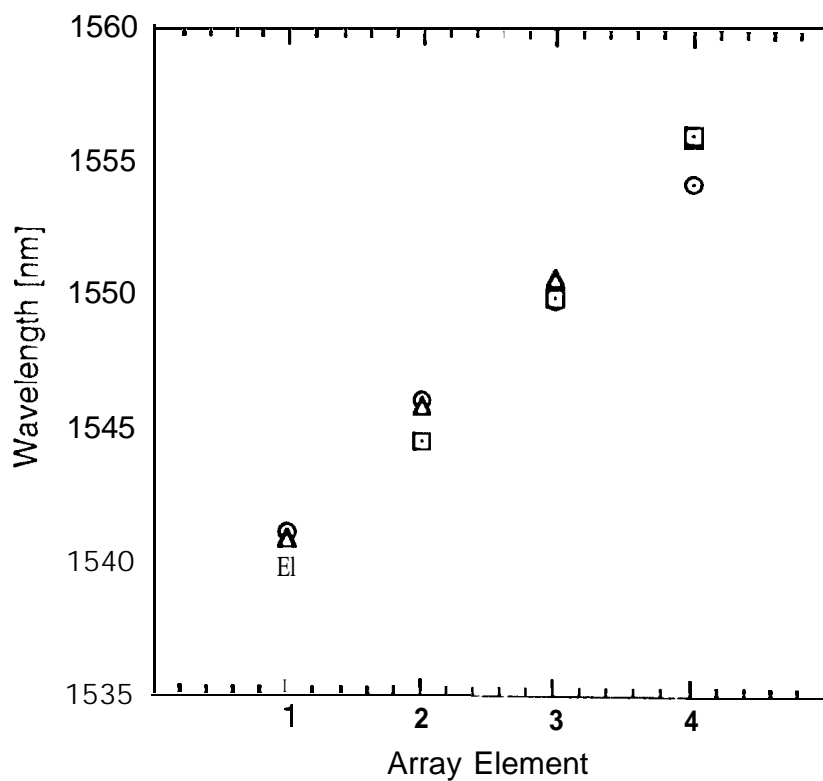


Figure 4. Emission wavelength versus array element for a few DFB laser arrays.

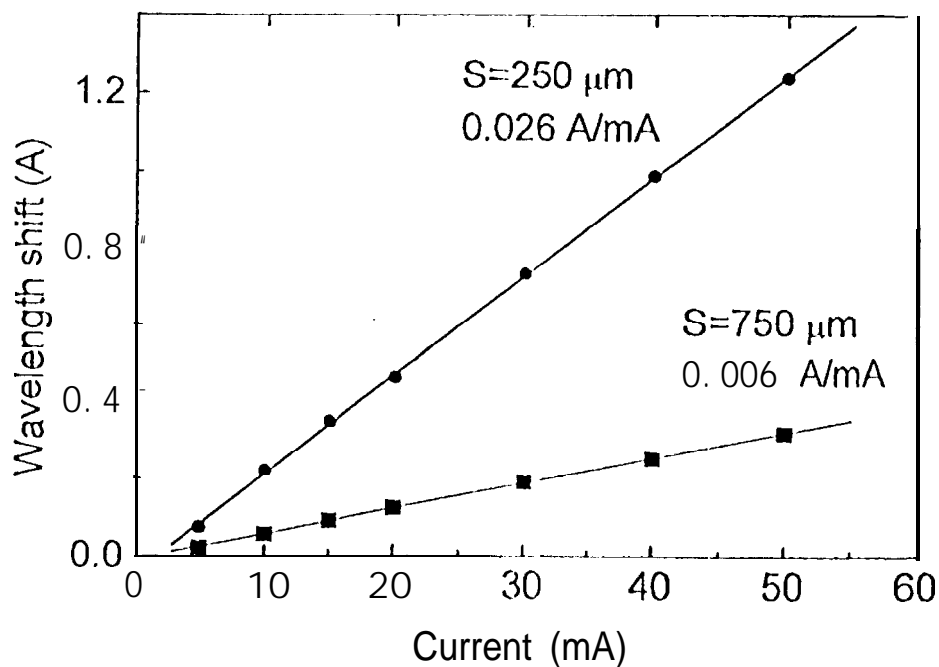


Figure 5. Effect of thermal crosstalk on the emission wavelength. S is the distance between the monitored device and the current swept device.

PREPUBLICATION REVIEW RECORD

INSTRUCTION: Check statement of circumstances applicable to this clearance and indicate action taken.

APPLICABLE CIRCUMSTANCE(S):

- 1. () A JPL "reportable item" is not disclosed but may exist or be "in the making." (NOTE: Originate Notice of New Technology).
2. () JPL or () JPL SubK unreported "reportable item" is disclosed. (NOTE: originate Notice of New Technology - if SubK, request NTR and decline clearance until NTR is received. Caltech and NRO to review for foreign filing when "item" is within a statutory class of patentable subject matter).
3. () Reported item of new technology is disclosed - U.S. Patent Application filed. (NOTE: look for reportable and/or patentable improvements. Ask NRO or Caltech for instructions if any are found).
4. (X) Reported item of new technology is disclosed - no U.S. Application filed. (NOTE: Look for new reportable subject matter for new NTR. If subject matter for new NTR is present, it should be prepared. If a patent application has been ordered or is in preparation, the new subject matter should be brought to the attention of the attorney as soon as possible and foreign filing review by Caltech and NRO is essential.
5. () JPL SubK invention, of other 3rd party invention, will be disclosed. (NOTE: Deny clearance unless written permission to publish has been obtained from invention owner).

ACTION TAKEN:

- (x) Talked with ___ Tel. ___
(x) Reviewed: () abstract () manuscript () title of publication only.
() Notice of New Technology originated - copy of clearance, abstract, manuscript or article put in case folder.
() Because this is not a JPL invention, written permission of invention owner for JPL publication has been confirmed,
() Foreign filing Review. Clearance approved by:

Handwritten signature and date 2/8/96, labeled NMO Rep. and Date.

Handwritten signature, labeled CIT Rep. and Date.

CLEARANCE: () Recommended () Conditional - see Comments () Delayed - see Comments

COMMENTS: The four element DFB Ridge Waveguide laser array fabrication and laser structures needs an NTR. It probably has patentable subject matter. An NTR has been requested.

PREPARED BY: Marianne S. Hanidi February 6, 1996